Connecting Changing Ocean Circulation with Changing Climate

Michael Winton, Stephen M. Griffies, Bonnie Samuels,

Geophysical Fluid Dynamics Laboratory/NOAA, Princeton, New Jersey

Jorge Sarmiento and Thomas L. Frölicher

Atmospheric and Oceanic Sciences, Princeton University

Submitted to *Journal of Climate*

DRAFT

14 May 2012

Corresponding author address: Michael Winton, NOAA/GFDL, Princeton University Forrestal Campus, 201 Forrestal Rd., Princeton, NJ 08540.
E-mail: Michael.Winton@noaa.gov

Abstract

The influence of changing ocean currents on climate change is evaluated by comparing an earth system model's response to increased CO_2 with and without an ocean circulation response. Inhibiting the ocean circulation response, by specifying a seasonally-varying preindustrial climatology of currents, has a much larger influence on the heat storage pattern than on the carbon storage pattern. The heat storage pattern without circulation changes resembles carbon storage (either with or without circulation changes) more than it resembles the heat storage when currents are allowed to respond. This is shown to be due to the larger magnitude of the redistribution transport – the change in transport due to circulation anomalies acting on control climate gradients – for heat than for carbon. The net ocean heat and carbon uptake are slightly reduced when currents are allowed to respond. Hence, ocean circulation changes potentially act to warm the surface climate. However, the impact of the reduced carbon uptake on radiative forcing is estimated to be small while the redistribution heat transport shifts ocean heat uptake from low to high latitudes increasing its cooling power. Consequently, global surface warming is significantly reduced by circulation changes. Circulation changes also shift the pattern of warming from broad northern hemisphere amplification to a more structured pattern with reduced warming at subpolar latitudes in both hemispheres and enhanced warming near the equator.

1. Introduction

Climate models project large changes in ocean circulation in response to increasing greenhouse gases. Atlantic meridional overturning circulation (AMOC) declines from 0% to more than 50% are projected for the 21st century (Solomon et al 2007). Southern ocean circulation response is also large and model dependent (Russell et al 2006). Gnanadesikan et al (2007) note large changes in tropical thermocline circulation in addition to AMOC and southern hemisphere circulation changes in three GFDL climate models. While the ocean's influence on surface climate changes is understood to occur through heat and carbon uptake, there is a lack of mechanistic understanding of these processes, including the role of the circulation response. Banks and Gregory (2006) show that the ocean heat storage pattern in a warming climate is quite different than that of a passive tracer with the same surface source. Xie and Vallis (2011) use an idealized ocean model to show that this difference is robust to various ocean model formulation and forcing differences. Both studies identify the redistribution of control climate ocean heat content as the important factor in the storage pattern differences (the passive tracer was absent in the control climate). However, by design these experiments cannot determine how this heat redistribution feeds back to alter the surface climate response. Winton (2003) showed that the impact of ocean circulation change might be substantial by uniformly varying the current speeds of an ocean circulation imposed on two climate models. Current speed increases produced high latitude warming and low latitude cooling and also increased global temperature.

In this study we address the role of ocean circulation changes by making an additional set of climate change simulations with a fully coupled Earth System Model. In addition to the standard control and CO_2 increase experiments, a corresponding pair of experiments (preindustrial control and increasing CO_2) are performed which fix the ocean circulation to a seasonally varying climatology based on the control experiment. The fixed-current response determined from this pair of experiments is used to divide the total response into two parts, one due to changing ocean circulation (the difference between the free- and fixed-current responses) and the other due to all other factors (the fixed-current response).

The model used and experimental design are described in the next section. Section three discusses the impact of the ocean circulation response on the distributions of heat and carbon storage in the ocean interior. The impact of the circulation response on the surface climate is presented in section four. The final section discusses the results.

2. Experiment design

The earth system model (ESM) used in this study is the GFDL ESM2M (Dunne et al 2012a; Dunne et al 2012b). The physical model is closely related to the GFDL CM2.1 model (Delworth et al 2007) used for the CMIP3 comparison. The responses of AMOC and global temperature are similar to those of CM2.1 (Winton et al 2012; Stouffer et al 2006). In this study we make use of 100-year 1%/year atmospheric CO_2 increase experiments to evaluate the response of the carbon cycle to increased atmospheric carbon

and of the climate to increased radiative forcing. Since atmospheric CO_2 is specified, we cannot directly evaluate the impact of differences in carbon uptake on climate change. Instead we will estimate the impact of such uptake on atmospheric CO_2 and radiative forcing.

We assess the role of changing currents on the simulated climate change by performing a pair (control and 1%/year CO_2 increase) of companion experiments where the ocean circulation is forced to follow a specified seasonal cycle. This climatology of currents is formed from the first 100 years of ESM2M's standard 1860 control experiment (following its long spin up). ESM2M uses a real freshwater flux boundary condition so mass balance requires that the surface water flux also be specified from this climatology. Although currents are specified in the fixed-current case, all parameterized subgrid mixing and convection processes operate on the evolving hydrography as in the standard prognostic model. A similar experimental setup was used by Winton (2003) to investigate the impact of ocean circulation on climate.

The fixed-current control experiences significant drift, warming by about 1K in the first 30 years from its free-current control initial condition. Therefore all fixed-current perturbation quantities are reported as differences between the fixed-current perturbation run and its control experiment. The analysis in this paper uses averages over years 81-100 of the experiment when the CO_2 level is, on average, about 2.4 times pre-industrial and the radiative forcing is 4.5 W/m^2.

3. Heat and carbon storage

3.1 Model results with fixed and free currents

Figure 1 compares the perturbation heat and dissolved inorganic carbon (DIC) column burdens in the fixed- and free-current experiments. The differences between the right and left panels reflect the influence of ocean circulation changes that are only allowed to operate in the free-current experiment depicted on the right. The centers of large carbon storage in the Southern Ocean, subtropical gyres and in the western North Atlantic are diminished by changing currents while the low values in the tropics are increased somewhat. By contrast with the modest differences in carbon storage, the heat storage pattern changes dramatically when allowing circulation change. In the free current case, a region of reduced heat content appears in the northern North Atlantic and GIN seas and a band of high storage appears just to the south along the North American coast. This dipole pattern is closely related to the AMOC subsurface temperature fingerprint (Zhang 2008) and indicates a weakening of the overturning. A new center of heat storage appears in the tropical Atlantic spreading east from the northeast coast of South America. A plume of increased heat storage streams east from South America at about 40S. The gyre storage pattern apparent in the fixed circulation heat storage and in the carbon storage of both experiments has been eliminated by circulation changes. Considering the four storage patterns, the heat storage with responding currents is qualitatively different from the other three. Furthermore, we note that the differences between the heat storage patterns are similar to the differences between passive anomaly temperature and heat storage in the Banks and Gregory (2006) experiments (see their Fig. 2). The fixed-current heat storage here shows pattern similarities with their passive anomaly

temperature which was, unlike heat, not present in the preindustrial ocean but was forced with the surface heat flux perturbation and experienced the evolving ocean circulation of their climate change experiment.

Figure 2 shows the zonal mean temperature and DIC change for the fixed- and free-current experiments. Again the carbon patterns are similar with small differences related to circulation changes. The weakening of the AMOC results in less DIC increase at high northern latitudes. With the exception of enhanced northern hemisphere warming in the subtropical gyres, the pattern of temperature changes under fixed currents resembles the DIC changes more than it resembles temperature change with free currents. In the deep ocean, the free-currents response has cooling high northern latitudes while at high southern latitudes it has increased warming relative to the fixed current case. The difference in Southern Ocean response is due to reduced convection which causes heat to accumulate beneath the surface. The fixed current case maintains high southern latitude convection and surface heat loss. The effect of maintained convection on carbon storage is opposite to heat – Southern Ocean carbon storage is larger in the fixed-current case. The maintenance of convection in the fixed-current case is difficult to attribute since, as noted earlier, surface freshwater fluxes are fixed at control values to achieve mass balance while heat fluxes interact with the changing climate.

At lower latitudes, the fixed- and free-current warming patterns are also very different. With free currents, lobes of deep warming appear at 40N and 40S, but the gyre warming equatorward of these features is eliminated. It is replaced by a weaker warming that

extends down to about 1 km depth, particularly in the tropics. A region of reduced warming appears near the equator at several hundred meters depth. As was the case for the column heat and carbon burdens, the temperature change pattern with free currents is more structured than the other three patterns.

3.2 Mechanism for storage pattern differences

Now we address the reason for the distinct appearance of the temperature response when ocean circulation is free to change relative to the carbon responses and the fixed-current temperature response. Aside from circulation, there are a number of reasons that carbon storage might differ from heat storage: differing surface histories (exponentially increasing in the case of carbon); atmospheric carbon is globally well mixed unlike surface warming; carbon uptake is subject to solubility and carbonate chemistry while surface temperature anomalies are influenced by radiative damping to space from the atmosphere/mixed-layer system. However, these differences apply to the temperature and carbon fixed-current responses which were shown to be largely similar (Figs. 1 and 2).

The climate model ocean age tracer gives insight into the differing distributions of heat and carbon storage in the free-currents case. The age tracer is set to zero in the mixed layer and increases with time (i.e. at rate of 1 year/year) so that it measures the time since a water parcel was last ventilated at the surface. The age tracer is spun up for several thousand years in the control experiment. Anti-correlation between control ocean age and heat or carbon storage would indicate these tracers are taken up by the simple process

of exposure to increasing surface values followed by transport into the interior, resulting in the oldest water having the least tracer. The control climate age tracer has a correlation with heat storage of -0.30 and with carbon storage of -0.83 in the upper kilometer of the world ocean in the free-currents case. This indicates that ventilation by control climate transport processes is much more important for explaining the carbon storage distribution than it is for heat storage.

The differing correlations of age tracer with the heat and carbon storage also imply that a changing circulation can have different impact on different tracers, in this case influencing heat more than carbon. Banks and Gregory (2006) showed that the difference between the storage of heat and a passive tracer with the same surface flux anomaly was due to a redistribution transport term which was absent for the passive tracer. Here we seek to quantify redistribution for tracers, such as heat and carbon, that are present in the preindustrial ocean and so have a redistribution term. Breaking a tracer, Q and velocity, **v** into control (subscript zero) and perturbation (primed) components, the perturbation Q transport is:

$$(\mathbf{v}Q)' = \mathbf{v}Q - \mathbf{v}_0Q_0 = \mathbf{v}'Q_0 + \mathbf{v}_0Q' + \mathbf{v}'Q' \qquad (1)$$

The first term in the rightmost expression is the redistribution transport which is due to the circulation change operating on the control climate tracer field. This term was missing in the equation for the Banks and Gregory passive anomaly temperature since that tracer does not exist in the ocean prior to the climate perturbation. It is this absence

of initial structure rather than the passive/active distinction that accounted for the distribution difference. In the fixed-current experiments done here, the third term on the right side of (1) has also been eliminated since **v**'=**0**. Additionally, the fixed- and free-current experiments do not have the same perturbation surface heat flux. We will show later that these terms are smaller than the redistribution transport. Therefore the similarity of our fixed-current heat storage with the Banks and Gregory passive anomaly temperature storage comes about because the redistribution term is eliminated – here by fixing the circulation (**v**'=0) and in Banks and Gregory by eliminating the preindustrial gradients (Q_0=0).

Carbon, of course, existed in the ocean prior to anthropogenic emissions but the relative importance of the redistribution terms for heat and carbon depends upon the relative magnitude of the pre-industrial range and the surface perturbation. To see this we define a new non-dimensional number, the redistribution number, R_Q, as the ratio of the two first order terms on the right side of (1), the redistribution transport term ($\mathbf{v}'Q_0$) and the fixed-current transport term ($\mathbf{v}_0Q'$):

$$R_Q = (Q_0/Q')\,(v'/v_0) \qquad (2)$$

where the symbols are now reinterpreted as scales for the fields rather than the 4-dimensional climatological fields themselves. The fractional change in circulation, v'/v_0, appears in both the redistribution numbers for temperature, R_T, and carbon, R_C, and so does not affect their comparison, which hinges instead on the relative magnitudes of

T_0/T' and C_0/C'. Scales for these terms could be assigned in a number of different ways. We have chosen to use the range of horizontally averaged tracer values in the preindustrial climate as Q_0 and the surface perturbation as Q'. Figure 3 shows horizontally averaged temperature and dissolved inorganic carbon profiles for the four experiments that are used to obtain these scales. The preindustrial gradient of temperature (T_0~16 K) is an order of magnitude larger than the surface perturbation (T'~1.3 K) while for carbon, the preindustrial gradient (C_0~320 μmol/kg) is about twice the perturbation (C'~160 μmol/kg). Therefore the preindustrial gradient, relative to the surface perturbation, is much larger for temperature than for carbon. Evaluating the Q_0/Q' ratios in (2) the redistribution numbers for the two quantities are:

$$R_T \sim 12\ v'/v_0 \qquad \text{and} \qquad R_C \sim 2\ v'/v_0 \qquad (3)$$

Considering that the ocean contains about 60 times more carbon than the atmosphere, it may seem surprising that an atmospheric carbon perturbation of a little more than a doubling can impress the large surface DIC change relative to the gradient seen in Fig. 3. This is because of the smallness of the preindustrial DIC gradient. Although the ocean has a large carbon content, the range of DIC values is only a small fraction of the mean.

The fact that R_T is six times larger than R_C shows that the redistribution term is relatively much more important in the transport term of the temperature equation. To evaluate the absolute importance of redistribution for either temperature or carbon transport we must estimate the v'/v_0 ratio. One way to do this is to take the square root of the ratio of total

ocean perturbation and control circulation kinetic energies. This gives $v'/v_0 \sim 0.3$ and, using (3), $R_T \sim 3.6$ and $R_C \sim 0.6$. Redistribution transport dominates the perturbation temperature transport but is less important, although not negligible, for carbon. Transient tracers such as CFCs or bomb ^{14}C have redistribution numbers of zero since they did not exist in the preindustrial ocean. In terms of the relative importance of redistribution transport, carbon is closer to these transient tracers than it is to temperature.

To complete the scale analysis of (1), we note that the terms T_0/T' and C_0/C' scale the ratios of the redistribution term to the higher-order terms – the third terms on the right side. The values given in (3) indicate that $v'T'$ is about 1/12 and $v'C'$ is about ½ of their corresponding redistribution terms. Summarizing these scales, the redistribution, fixed-current transport and higher-order terms are in rough proportions 1 : 0.3 : 0.1 for temperature and 1 : 1.6 : 0.5 for carbon. The dominance of the redistribution term in the perturbation temperature equation is an important consideration when comparing simulated and observed ocean heat storage. The scaling here suggests that circulation changes should leave fingerprints on the observed pattern.

A more direct way to compare the heat and carbon redistribution terms that gives insight into the global nature of the redistribution is depicted in the top panel of Fig. 4. Here the northward redistribution transports in (1) are roughly estimated by applying the meridional velocity changes, averaged over year 81-100, to the control climate temperatures and DIC values. These estimates are then divided by their respective global net surface fluxes to obtain non-dimensional quantities for comparison. The estimated

redistribution transport of heat is seen to be of the same order as the perturbation surface flux while that of carbon is an order of magnitude smaller. Consistent with the above scaling analysis, circulation changes induce a much larger scaled heat transport than carbon transport. The redistribution heat transport shows large divergences poleward of 40° north and south and a large convergence near the equator. The divergence of heat out of northern subpolar regions is caused by the weakening of the AMOC (Rugenstein et al 2012). A similar feature in the south is associated with large changes in both the overturning and barotropic flow linked to a strengthening and poleward shifting of the westerlies and reduced Antarctic Bottom Water formation. The redistribution convergence of heat near the equator is due to reduced tropical upwelling as described by Gnanadesikan et al (2007). This feature is associated with tropical warming, in and below the thermocline, in all three ocean basins. The dominant feature of the carbon redistribution transport is equatorial divergence due to reduced upwelling of carbon rich water.

4. Surface fluxes and climate response

In addition to redistributing heat storage, circulation changes alter the distribution of surface heat fluxes. Table 1 lists downward surface heat flux perturbations at high and low latitude for the two experiments. About ½ of the heat uptake occurs between 40S and 40N in the fixed current experiment but this is reduced to about ¼ when ocean circulation is allowed to respond. The difference between the free- and fixed-current runs shows that heat uptake is reduced at low latitudes and increased at high latitudes, particularly in the north, as a result of circulation changes. This shift is a response to the

redistribution heat transport. Part of the redistribution transport results in storage changes or is counteracted by other transports. However a substantial fraction of the redistribution transport is uncompensated by these factors and drives the surface flux changes evident in Table 1. The lower panel of Fig. 4 compares the northward redistribution heat transport (divided by three, for comparison purposes) to the surface flux difference between the free- and fixed current runs integrated from the southern boundary. Coincidence of these curves would indicate that 1/3 of the redistribution transport divergence is compensated by surface flux change. The closeness of the comparison supports the role of the redistribution heat transport as a driver of surface heat uptake redistribution from low to high latitudes.

This meridional shift of heat uptake induced by ocean circulation changes has significant impact on the pattern of SST change. Fig. 5 shows the SST change for fixed- and free-current experiments. The fixed-current pattern has substantially greater warming at subpolar latitudes in both hemispheres, particularly in the North Atlantic where the patch of SST cooling associated with AMOC weakening is replaced by a weak minimum in warming. Deep mixed layers that are maintained with fixed currents produce only a modest dilution of the surface warming in this region. The warming impact of maintained circulation on high northern latitudes is consistent with the comparison by Rugenstein et al (2012) of climate change in models with large and small AMOC declines. That study showed that the models with large declines had reduced high northern latitude warming due to the reduced transport of heat by the AMOC into this region which increased ocean heat uptake there.

At lower latitudes the fixed-current pattern has broad Northern Hemisphere amplification while the free-current pattern has a band of enhanced warming along the equator. A robust enhanced equatorial response in climate change experiments was first noted by Liu et al (2005). The pattern appears in both transient and equilibrium responses of GFDL CM2.1 which is closely related to ESM2M (Xie et al 2010). The fixed-current experiment shows that ocean circulation changes are necessary for the appearance of this pattern in the transient response. Hints of the enhanced equatorial response can be seen in the fixed-current SST change but they are embedded in a broader reduction in warming due to maintenance of deep upwelling in this experiment.

We have examined the patterns of heat and carbon storage and SST change. Now we assess the impact of circulation changes on the overall magnitude of climate change as indexed by the global mean surface temperature. The experimental design we have used, with specified atmospheric CO_2 concentrations, forces us to make the assessment of the influence of carbon uptake indirectly. We can gauge the impact of the ocean circulation through carbon by calculating the impact the differential uptake would have on atmospheric CO_2 levels, had it remained in the atmosphere, and from there on radiative forcing.

The ocean carbon storage is 16.9 Pg less in the free-currents experiment relative to the fixed-current case in the year 81-100 average. If this carbon had all remained in the atmosphere, the pCO_2 would have been increased by 8 ppm above the actual value of

about 700 ppm at nominal year 90. Thus the additional increase from ocean circulation change is a little over 1%. This amounts to one year of radiative forcing increase in this 1%/year CO_2 increase experiment. Since 90 years of these increases sum to the year 81-100 year average forcing, the additional radiative forcing from reduced carbon uptake would be relatively very small. This is consistent with Friedlingstein et al. (2006). Based on the results of eleven different carbon cycle-climate models, they found that the ocean uptake is reduced by about 20Pg/K due to climate change. With the 2K warming in ESM2M this feedback would reduce carbon uptake by about 40 Pg and increases radiative forcing by 2-3%.

The impact of heat uptake differences can be directly assessed: the global warming is 27% less in the free-current case (Table 2) over the years 81-100. This substantial warming reduction occurs in spite of a small reduction in ocean heat uptake accompanying the circulation changes over the same period. The standard interpretive model for global temperature response, ΔT, in terms of radiative forcing, F and heat uptake, N is (Cubasch et al 2001):

$$F = \lambda \Delta T + N \qquad (4)$$

where λ is the climate feedback parameter. On the decade-to-century timescales of interest the heat uptake, N, is dominated by warming of the ocean below the mixed layer. Therefore (4) expresses a balance between the radiative forcing source of energy and the sum of the dissipative fluxes to space, $\lambda \Delta T$, and into the deep ocean, N. The temperature

perturbation is determined from this forced-dissipative balance which neglects the warming of the atmosphere/ocean mixed layer system since it has negligible heat capacity on the decadal timescales of interest. Making the usual assumption that ocean circulation does not affect the equilibrium (N=0) response, both fixed- and free-current models have the same equilibrium climate feedback parameter, λ. Therefore (4) does not allow for the free-current experiment to have both a smaller temperature response and a smaller ocean heat uptake.

This problem can be resolved by making use of the concept of ocean heat uptake efficacy introduced by Winton et al (2010). Efficacy factors have previously been applied to radiative forcings to account for differences in their global temperature responses per W/m^2 forcing. For example, Hansen and Nazerenko (2004) found that a soot on snow radiative forcing induced about twice the warming of the same radiative forcing applied through increased CO_2, giving soot-on-snow forcing an efficacy of 2. Hansen et al (1997) showed that forcings that are focused at the surface and at high latitudes have larger efficacies (i.e. they induce larger temperature responses). Consistent with this finding, Winton et al (2010) showed that ocean heat uptake in GFDL CM2.1 occurred preferentially at subpolar latitudes and had a larger temperature impact than CO_2. They modified (4) to apply an efficacy factor, ε, to the heat uptake:

$$F = \lambda \Delta T + \varepsilon N \qquad (5)$$

This equation resolves the problem that the transient climate response generally does not scale up to the equilibrium response (ΔT_{EQ}) by applying a factor of F/(F-N) as would be expected if radiative forcing and heat uptake had equivalent influence. For most models scaling up the transient response leads to an effective sensitivity, $\Delta T_{EF} = \Delta T \cdot F/(F-N)$ that is less than ΔT_{EQ}. Consistent with this, a number of transient simulations find the effective sensitivity increasing over time as the heat uptake declines. Winton et al (2010) show that (5) accounts for this behavior and produces the apparent time-dependence of sensitivity with constant parameters.

Equation (5) is used to diagnose efficacy from radiative forcing, heat uptake and transient and equilibrium warming. The terms in (5) for the fixed- and free-current experiments are listed in Table 2. In the fixed-current case, the efficacy is 1 indicating that the heat uptake has the same influence on surface temperature as CO_2 forcing. The increase in efficacy from 1 to 1.6 that occurs when currents are free to respond is consistent with the shift in heat uptake from low to high latitudes discussed earlier and the sensitivity study of Hansen et al (1997) showing that such a shift should increase efficacy. Summarizing, it is the shift in location of heat uptake to regions of greater sensitivity rather than a change in heat uptake magnitude that gives the ocean circulation response its large mitigating influence on transient global warming.

5. Conclusions

In this study we have evaluated the influence of changing ocean currents on climate change by comparing an ESM's response to increased CO_2 with and without an ocean

circulation response. Inhibiting the ocean circulation response, by specifying a seasonally varying climatology of currents, had a much larger influence on the heat storage pattern than on the carbon storage pattern. Heat storage without circulation changes resembled carbon storage (either with or without circulation changes) more than it resembled the heat storage when currents are allowed to respond. This result was shown to be due to the larger magnitude of the redistribution transport – the change in transport due to circulation anomalies acting on control climate gradients – for heat than for carbon.

The overall uptake of heat and carbon were slightly reduced when currents were allowed to respond potentially giving circulation changes an additional warming effect. However, the impact of the reduced carbon uptake on radiative forcing was estimated to be minimal while the redistribution heat transport shifted heat uptake from low to high latitudes increasing its cooling power. Consequently, global warming was significantly reduced by circulation changes. Circulation changes also shifted the pattern of warming from broad northern hemisphere amplification to a more structured pattern with reduced warming at subpolar latitudes and enhanced warming near the equator.

Since ocean circulation response varies among climate models and, as was shown here, influences the transient response, it contributes some of the uncertainty in that response. Although we have demonstrated that the circulation response induces large changes in the surface temperature response in GFDL ESM2M, it remains to be seen how influential the *differences* in circulation responses between models are on their surface temperature

response differences. Should the influence prove to be significant, the pattern of heat storage, which we have argued fingerprints the circulation response, should place an observational constraint on that influence. The simulated impact of ocean circulation itself on surface climate was shown to be model dependent due to differing radiative feedbacks by Winton (2003), so the usefulness of the circulation constraint on the transient climate response must still be established. Nevertheless, this approach represents a pathway to reduced uncertainty with distinctly different opportunities for progress than those for resolving uncertainties in radiative feedbacks.

Acknowledgments

The authors thank John Dunne, Isaac Held, and Geoff Vallis for helpful reviews of the manuscript.

References

Banks, H. T., and J. M. Gregory, 2006: Mechanisms of ocean heat uptake in a coupled climate model and the implications for tracer based predictions of ocean heat uptake, *Geophys. Res. Lett.*, **33**, L07608, doi:10.1029/2005GL025352.

Cubasch, U. and Coauthors, 2001: Projections of future climate change. *Climate change 2001: The Scientific Basis. Contribution of Working Group I to the Third Assessment Report of the IPCC*, J.G. Houghton et al, Eds., Cambridge University Press, 525-582.

Delworth, T.L., and Coauthors, 2006: GFDL's CM2 Global Coupled Climate Models. Part I: Formulation and Simulation Characteristics, J. Climate, 19(5), DOI:10.1175/JCLI3629.1.

Dunne, J.P., J.G. John, A.J. Adcroft, S.M. Griffies, R.W. Hallberg, E.N. Shevliakova, R.J. Stouffer, W. Cooke, K.A. Dunne, M.J. Harrison, J.P. Krasting, H. Levy, S.L. Malyshev, P.C.D. Milly, P.J. Phillipps, L.A. Sentman, B.L. Samuels, M.J. Spelman, M. Winton, A.T. Wittenberg, N. Zadeh, 2012a: GFDL's ESM2 global coupled climate-carbon Earth System Models Part I: Physical formulation and baseline simulation characteristics, J. Climate, in press.

Dunne, J.P., J.G. John, R.W. Hallberg, S.M. Griffies, E.N. Shevliakova, R.J. Stouffer, J.P. Krasting, L.A. Sentman, P.C.D. Milly, S.L. Malyshev, A.J. Adcroft, W.Cooke, K.A.

Dunne, M.J. Harrison, H. Levy, B.L. Samuels, M. Spelman, M. Winton, A.T. Wittenberg, P.J. Phillips, N. Zadeh, 2012b: GFDL's ESM2 global coupled climate-carbon Earth System Models Part II: Carbon system formulation and baseline simulation characteristics, in prep.

Friedlingstein, P., and Coauthors, 2006: Climate–Carbon Cycle Feedback Analysis: Results from the C4MIP Model Intercomparison. *J. Climate*, **19**, 3337–3353.

Gnanadesikan, A., J. L. Russell, and F. Zeng, 2007: How does ocean ventilation change under global warming? Ocean Science, 3(1), 43-53.

Hansen, J., and L. Nazarenko, 2004: Soot climate forcing via snow and ice albedos. Proc. Natl. Acad. Sci. , 101, 423-428, doi:10.1073/pnas.2237157100.

Hansen, J., M. Sato, and R. Ruedy, 1997: Radiative forcing and climate response. *J. Geophys. Res*., **102**, D6, 6831-6864.

Liu, Z., S. Varvus, F. He, N. Wen, and Y. Zhong, 2005: Rethinking tropical oceanic response to global warming: The enhanced equatorial warming. *J. Climate*, **18,** 4684–4700.

Rugenstein, M.A.A., M. Winton, R.J. Stouffer, S.M. Griffies, and R. Hallberg, 2012: Northern high latitude heat budget decomposition and transient warming, revised for *J. Climate*.

Solomon, S., D. Qin, M. Manning, Z. Chen, M. Marquis, K.B. Averyt, M. Tignor and H.L. Miller (eds.), 2007: Contribution of Working Group I to the Fourth Assessment Report of the Intergovernmental Panel on Climate Change, 2007, Cambridge University Press, Cambridge, United Kingdom and New York, NY, USA.

Stouffer, R.J., T.L. Delworth, K.W. Dixon, R. Gudgel, I.M. Held, R.S. Hemler, T.R. Knutson, M.D. Schwarzkopf, M.J. Spelman, M. Winton, A.J. Broccoli, H-C. Lee, F. Zeng, and B.J. Soden, 2006: GFDL's CM2 Global Coupled Climate Models. Part IV: Idealized Climate Response. J. Climate, 19(5), DOI:10.1175/JCLI3632.1.

Winton, M., A. Adcroft, S.M. Griffies, R.W. Hallberg, R.J. Stouffer, 2012: Influence of ocean model formulation on simulated climate sensitivities, submitted to *J. Climate*.

Winton, M., K. Takahashi, and I.M. Held, 2010: Importance of ocean heat uptake efficacy to transient climate change, J. Climate, 23(10), 2333-2344.

Winton, M., 2003: On the climatic impact of ocean circulation. J. Climate, 16(17), 2875-2889.

Xie, P., and Vallis, G.K., 2011: The passive and active nature of ocean heat uptake in idealized climate change experiments, *Climate Dynamics*, DOI 10.1007/s00382-011-1063-8.

Xie, S.-P., C. Deser, G.A. Vecchi, J. Ma, H. Teng, and A.T. Wittenberg, 2010: Global warming pattern formation: Sea surface temperature and rainfall. *J. Climate*, **23**, 966-986.

Zhang, R., 2008: Coherent surface-subsurface fingerprint of the Atlantic meridional overturning circulation. Geophysical Research Letters, 35, L20705, DOI:10.1029/2008GL035463.

List of Tables

Table 1. Heat uptake (year 81-100 mean) by region in free-currents and fixed-currents experiments (10^{15} W).

Table 2. Evaluation of transient climate response (year 81-100 mean) using equation 5: Temperature change T (K), in terms of radiative forcing, F (W/m^2), equilibrium climate feedback parameter, λ ($W/m^2/K$), ocean heat uptake efficacy, ε and ocean heat uptake, N (W/m^2).

List of Figures

Fig. 1. Column heat (top) and dissolved inorganic carbon (bottom) content change (year 81-100 mean) for experiments with specified climatological currents (left) and freely evolving currents (right). Heat contents are in $(W/m^2)\cdot 90$ years. Carbon contents are in $moles/m^2$.

Fig. 2. Zonal mean temperature (top) and dissolved inorganic carbon (bottom) change (year 81-100 mean) for experiments with specified climatological currents (left) and freely evolving currents (right). Temperature changes are in K; dissolved inorganic carbon changes are in $\mu mole/m^3$.

Fig. 3. Horizontally averaged temperature (left) and dissolved inorganic carbon (right) for control (black) and perturbation (red) experiments averaged over years 81-100.

Fig. 4. Northward redistribution transport of heat and carbon normalized by their respective net surface fluxes (top). Northward redistribution transport of heat (divided by 3) and downward surface heat flux difference between free-currents and fixed-currents experiments integrated from southern boundary (bottom).

Fig. 5. Surface temperature change (year 81-100 mean) for specified climatological currents (left) and freely evolving currents (right) experiments (K).

Table 1. Heat uptake (year 81-100 mean) by region in free-currents and fixed-currents experiments (10^{15} W).

Heat uptake (PW)	**90S-40S**	**40S-40N**	**40N-90N**
Free-currents	.33	.18	.25
Fixed-currents	.28	.42	.13
Difference	.05	-.24	.11

Table 2. Evaluation of transient climate response (year 81-100 mean) using equation 5: Temperature change T (K), in terms of radiative forcing, F (W/m^2), equilibrium climate feedback parameter, λ ($W/m^2/K$), ocean heat uptake efficacy, ε and ocean heat uptake, N (W/m^2).

Experiment	**F =**	**λ**	**T +**	**ε**	**N**
VAR	4.5		1.9	1.6	1.5
FIX	4.5		2.6	1.0	1.6

Fig. 1. Column heat (top) and dissolved inorganic carbon (bottom) content change (year 81-100 mean) for experiments with specified climatological currents (left) and freely evolving currents (right). Heat contents are in $(W/m^2)\cdot 90$ years. Carbon contents are in $moles/m^2$.

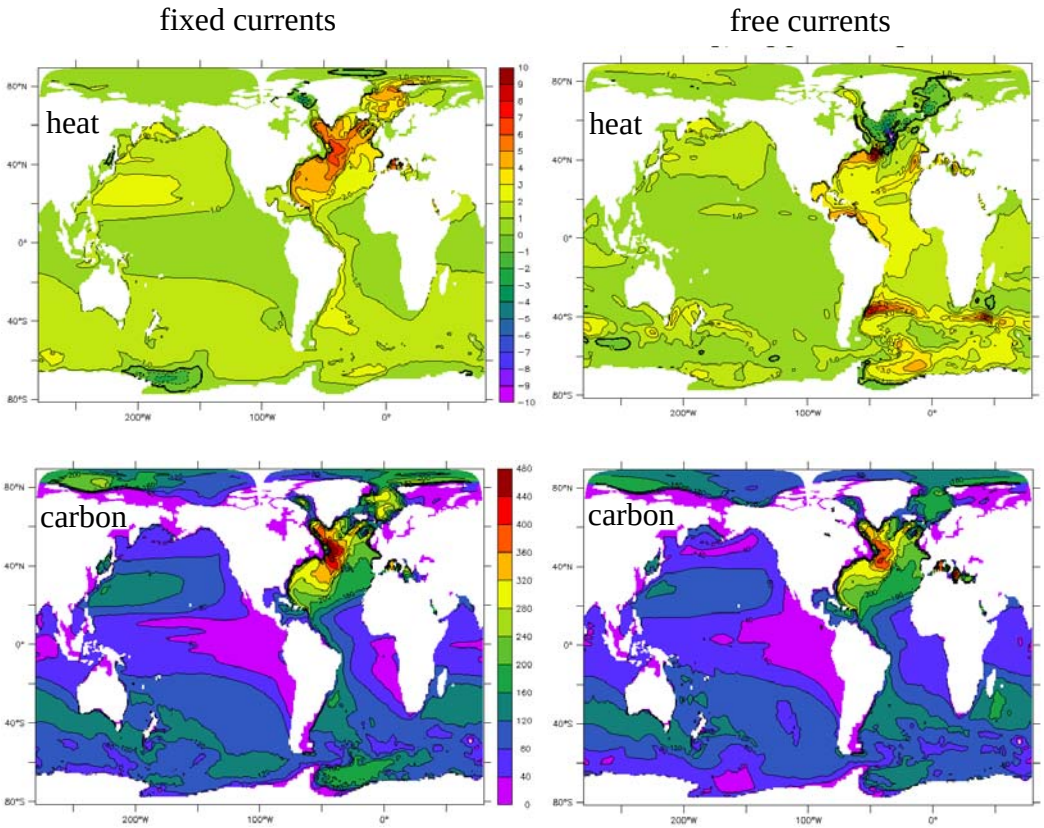

Fig. 2. Zonal mean temperature (top) and dissolved inorganic carbon (bottom) change (year 81-100 mean) for experiments with specified climatological currents (left) and freely evolving currents (right). Temperature changes are in K; dissolved inorganic carbon changes are in μmole/m^3.

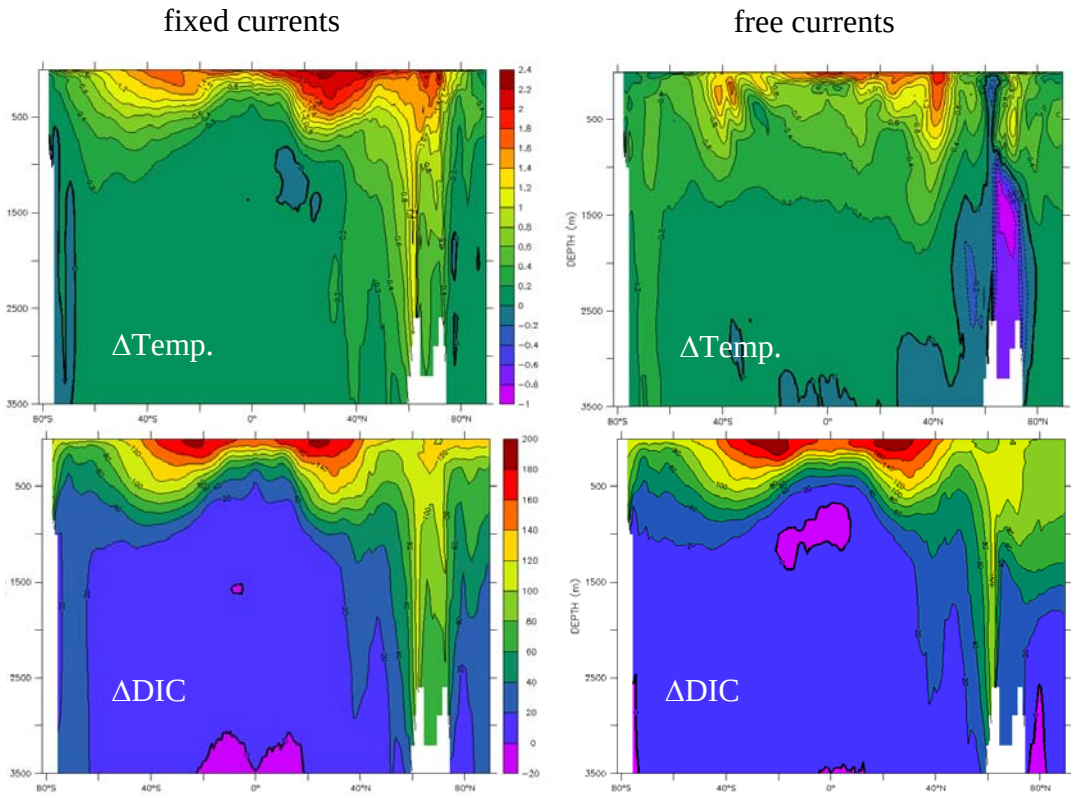

Fig. 3. Horizontally averaged temperature (left) and dissolved inorganic carbon (right) for control (black) and perturbation (red) experiments averaged over years 81-100.

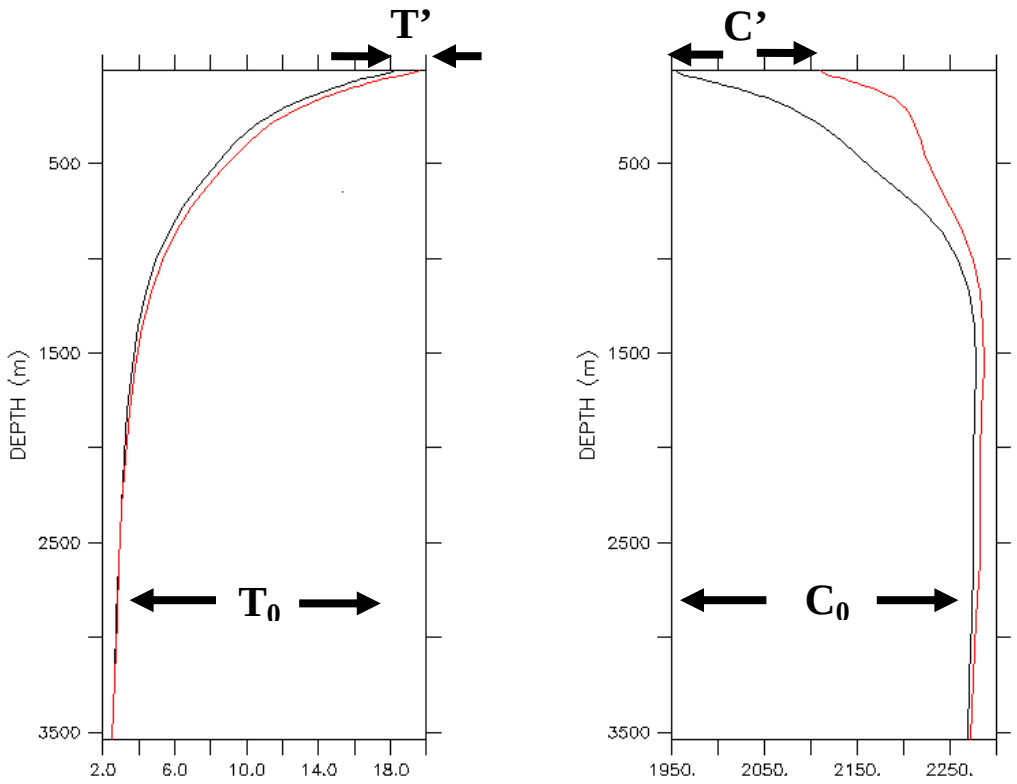

Fig. 4. Northward redistribution transport of heat and carbon normalized by their respective net surface fluxes (top). Northward redistribution transport of heat (divided by 3) and downward surface heat flux difference between free-currents and fixed-currents experiments integrated from southern boundary (bottom).

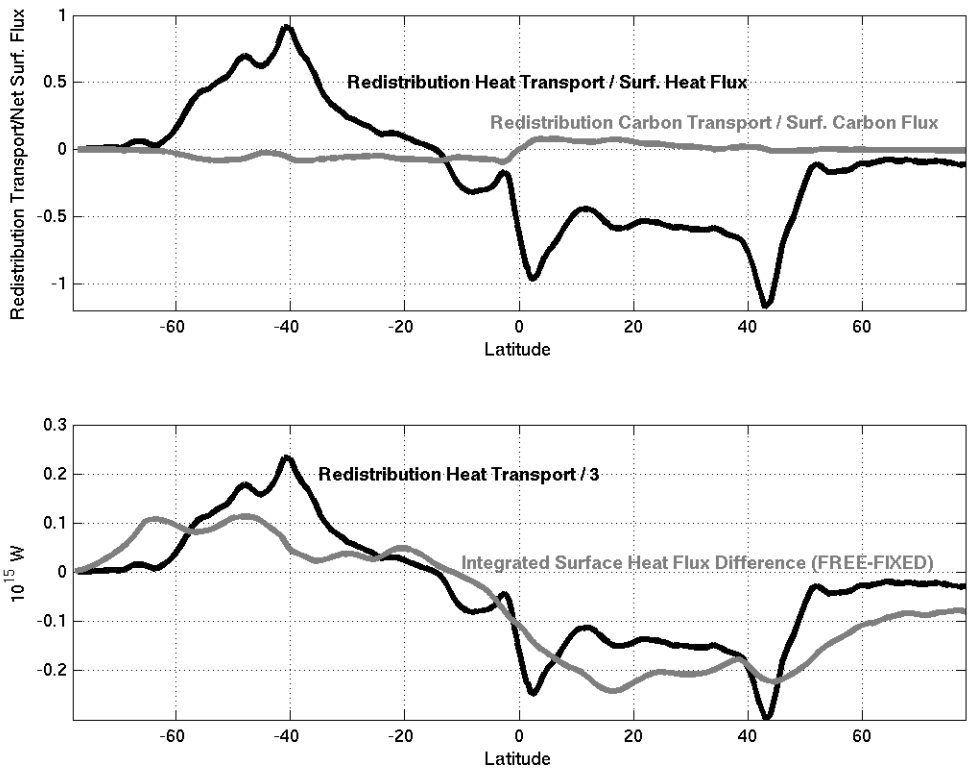

Fig. 5. Surface temperature change (year 81-100 mean) for specified climatological currents (left) and freely evolving currents (right) experiments (K).
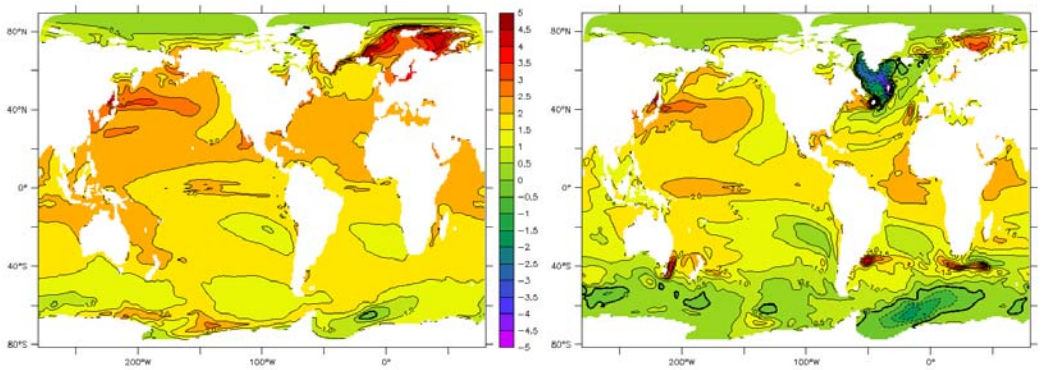
fixed currents free currents